Skew Characteristics of Image Fiber for High-Speed 2-D Parallel Optical Data Link

Moriya Nakamura, *Member, IEEE*, Toshimichi Otsubo, and Ken-ichi Kitayama, *Senior Member, IEEE*

***Abstract*—Skew of an image fiber, which has more than ten thousands of cores in a common cladding, was measured by a novel measurement method for the first time. This method can measure the time-of-flight difference between individual cores over the whole area of an image circle. The measurement result reveals that a test 100-m-long image fiber has skew of 5 ps/m, and the time-of-flight distributes randomly in the whole area of the image circle due to nonuniformity of the core dimension. It is also experimentally shown that the skew of an image fiber increases by bending. The theoretical analysis reveals that the bending-induced skew depends neither on the radius of curvature nor the shape of the curve but it depends only on the number of turns it is wound. The numerical calculation of skew by using typical parameters of image fibers shows that the winding have to be restricted to less than five turns to achieve a transmission speed of over 1 Gb/s/ch. Finally, we propose a twisted image fiber and an "8-shaped" bobbin to suppress the skew due to bending.**

***Index Terms*—Image fiber, optical interconnects, skew, two–dimensional (2-D) parallel transmission.**

I. Introduction

PARALLEL optical interconnection is an important technique for high-performance computing and switching systems because its high-speed optical transmission without parallel/serial data conversion enables an increased data throughput. There have been many reports on parallel optical interconnection modules using fiber ribbons and one-dimensional (1-D) laser diode (LD)/photodiode (PD) arrays. However, for massively parallel processing systems using smart pixel technology, whose structure is a two-dimensional (2-D) processor array, 2-D parallel optical interconnect is essential because the data to be transmitted are 2-D [1]. Additionally, the 2-D parallel technique can dramatically increase transmission channels in comparison with the 1-D parallel interconnects. 2-D parallel optical interconnects have been studied mainly in the area of free-space optical interconnects using lens systems [2], [3]. However, lens systems are not flexible in system implementations because the arrangement of each component is restrained by lens parameters such as focal length and, especially, it is difficult to apply them to interprocessor-board and intercabinet interconnections.

Manuscript received December 21, 1999; revised May 22, 2000.

M. Namakura and T. Otsubo are with the Communications Research Laboratory, Ministry of Posts and Telecommunications, Tokyo 184-8795, Japan (e-mail: moriya@crl.go.jp).

K. Kitayama was with the Communications Research Laboratory, Ministry of Posts and Telecommunications, Japan. He is now with the Department of Electronics and Information Systems, Osaka University, 2-1 Yamadaoka, Suita, Osaka 565-0871, Japan (e-mail: kitayama@comm.eng.osaka-u.ac.jp).

Publisher Item Identifier S 0733-8724(00)08083-X.

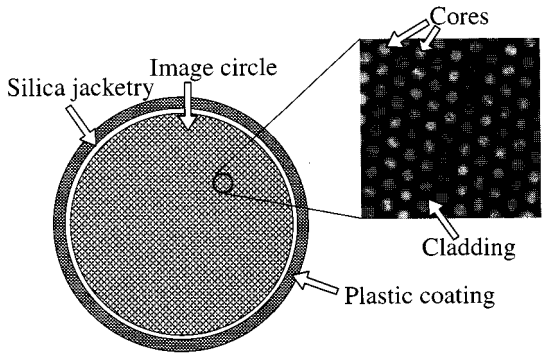

Fig. 1. Cross-sectional view of an image fiber.

We have been studying fiber-based 2-D parallel optical interconnects, especially ones using image fibers. We have reported experimental demonstrations of image-fiber-based optical interconnects with a novel multiplexing scheme, namely, space-code division multiple access (space-CDMA) [4]–[7]. Fig. 1 shows a cross-sectional view of an image fiber. Image fibers have been used as a direct-image transmission medium for, e.g., medical endoscopy and industrial inspection. An image fiber has several thousands to several tens of thousands of cores in a common cladding, and it can transmit 2-D optical signals in parallel. The typical dimensions are 3 μm in core diameter, 5 μm in spacing between cores, 800 μm in image diameter, etc.

One of the most important parameters of parallel optical transmission media is skew. Skew is defined as the maximum difference of propagation time between transmission channels, and it limits synchronous parallel transmission speed. In intercabinet interconnections, which need a transmission distance of up to 100 m, skew has to be less than 1 ps/m for a transmission speed of 1 Gb/s/ch [nonreturn to zero (NRZ} pulsewidth: 1 ns]. Some theoretical analyses of skew of fiber ribbons and attempts to fabricate low-skew fiber ribbons have been reported [8], [9]. However, skew of image fibers has not been well studied. One reason is that the conventional phase method [9], which is used to measure skew, cannot be suitably applied because an image fiber has so many cores and the core spacing is only a few micrometers.

In this paper, image fiber skew characteristics investigated by using a novel measurement method is reported for the first time. Section II describes the influence of time-of-flight difference between cores on optical pulses propagated through an image fiber. Section III presents a novel method for measuring the skew of image fibers. In Section IV, the measurement result is described, which reveals that a test 100-m-long image fiber

0733–8724/00$10.00 © 2000 IEEE

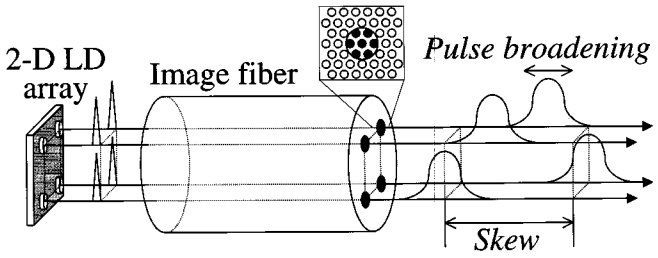

Fig. 2. Pulse broadening and skew caused by propagation delay difference between image-fiber cores.

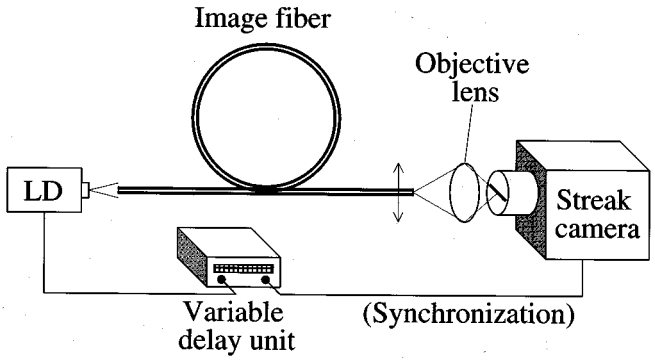

Fig. 3. Proposed skew measurement system.

having 3×10^4 cores has skew of 5 ps/m, and the time-of-flight distributes randomly in the whole area of the image circle. In Section V, it is shown both theoretically and experimentally that the skew of an image fiber is increased by bending. The bending-induced skew does not depend on the radius of curvature and the shape of the curve but only on how many turns it is wound. The numerical calculation shows that the winding must be restricted to less than five turns to achieve a transmission speed over 1 Gb/s/ch. Finally, we will propose a twisted image fiber and an "8-shaped" bobbin for suppressing skew due to bending.

II. Skew of Image Fibers

Fig. 2 schematically shows the propagation-delay difference on optical pulses propagated through an image fiber. Each optical pulse having a finite spot size broadens during the propagation in several cores because each core has a different propagation delay caused by fluctuations of relative refractive index and core diameter. Additionally, optical pulses arrive at the output end at different times because of uneven distribution of propagation delay over the whole image circle. This uneven distribution is caused by the residual stress as well as bending. To apply the image fiber to high-speed 2-D optical data link, we need to characterize both the local time-of-flight difference between individual cores in a small area and the global distribution of time-of-flight difference in the whole area of an image circle.

III. Novel Skew Measurement Method

The time-of-flight difference of fiber ribbons has been measured by using the phase method. The phase method compares the phase of each transmitted signal with that of a reference channel. However, this method is difficult to apply to image fibers because an image fiber has several tens of thousands of cores and the spacing between cores is only a few micrometers.

To the authors' knowledge, only one attempt to evaluate skew of image fibers has been reported by Kawai *et al.* [10]. The skew was evaluated from the broadened optical pulsewidth after the propagation through an image fiber by taking into account the mode dispersion. However, this method has some problems such as: i) inability to measure time-of-flight difference between individual cores, and ii) practical difficulty to measure distribution of time-of-flight difference in whole area of an image circle.

Fig. 3 schematically shows the proposed measurement method. An optical pulse is launched into all the cores of an image fiber. The output light of the image fiber is imaged on the front-end horizontal slit of the streak camera by an objective lens. The optical pulses which pass through the slit induce electrons on a photoelectric surface, and all the electrons are simultaneously swept vertically in the streak camera. The time-of-flight difference between the cores results in deviations along a vertical line. Thus all the optical pulses propagated through the cores imaged on a line along the slit are observed simultaneously on a real-time basis. The output endface of the fiber is scanned by moving in the vertical direction in order to measure the image circle area. This measurement method will resolve the problems i) and ii) described above. The precision of the measurement method is restricted only by the time resolution of the streak camera. The streak camera (Hamamatsu Photonics K. K., Model C5680) used in our experiment has a time resolution of 2 ps. The pulse jitter of the LD has the same influence on all the optical pulses propagated through the cores and, consequently, no influence on the relative propagation delay between the optical pulses. The jitter therefore does not effectively degrade the precision of the measurement.

IV. Experimental Results

By using the proposed method, we have measured the skew of an image fiber. The measured image fiber is 100 m long. It has 3×10^4 cores, and the picture diameter is 800 μm. The core diameter and the spacing are 3.0 and 4.4 μm, respectively. The materials of cores and cladding are silica glass. In the measurement, the image fiber was extended almost straight. Optical pulses of the LD was 59 ps in full-width at half-maximum (FWHM) at the wavelength of 650 nm. The cores are of multimode at this wavelength.

Fig. 4 shows the cores focused on a front-end slit, which was observed by a streak camera without sweep. Fig. 5 shows a streak camera trace of optical pulses propagated through 20 cores of the image fiber. The trace shows that there exists the time-of-flight difference between the observed cores. Each pulse has a trailing tail, which may be due to both the mode dispersion and the chromatic dispersion. The cores in the image fiber are aligned on the hexagonal close-packed (hcp) grids; therefore, the next row of the cores can be measured by vertically moving the image fiber observing the streak camera trace. The measured data can be plotted in a 2-D map of time-of-flight difference. Fig. 6 shows the 2-D plot of measured time-of-flight difference at the center of the image circle. The

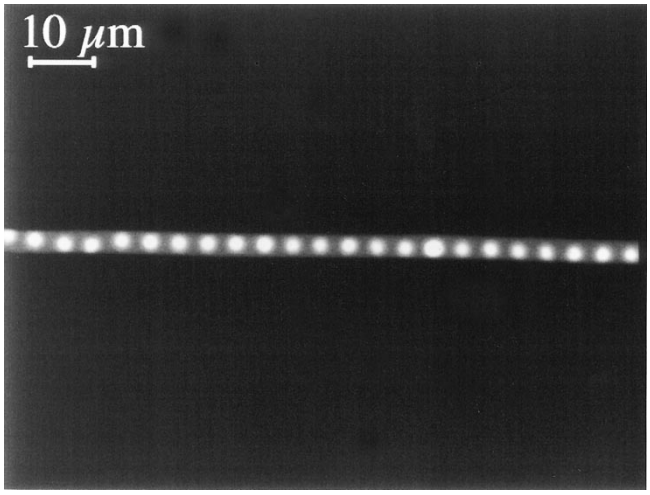

Fig. 4. Light spots cores imaged in a slit of a streak camera.

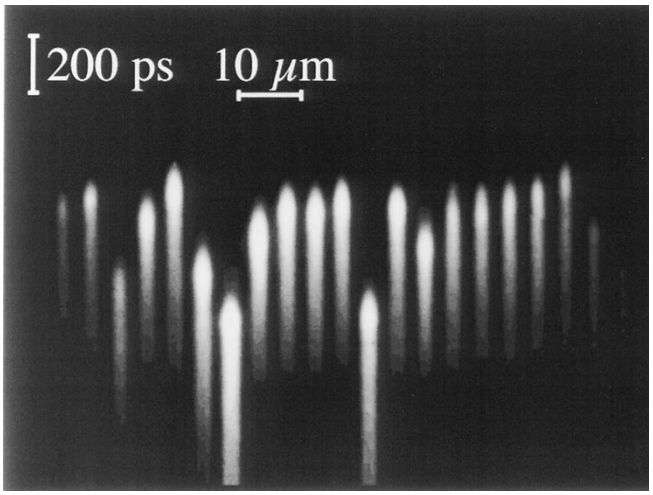

Fig. 5. Streak camera trace of optical pulses propagated through image fiber cores.

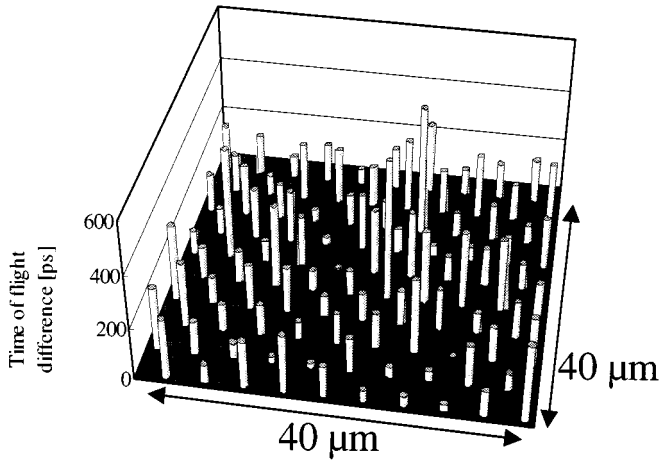

Fig. 6. Time-of-flight difference around the center of the test image fiber.

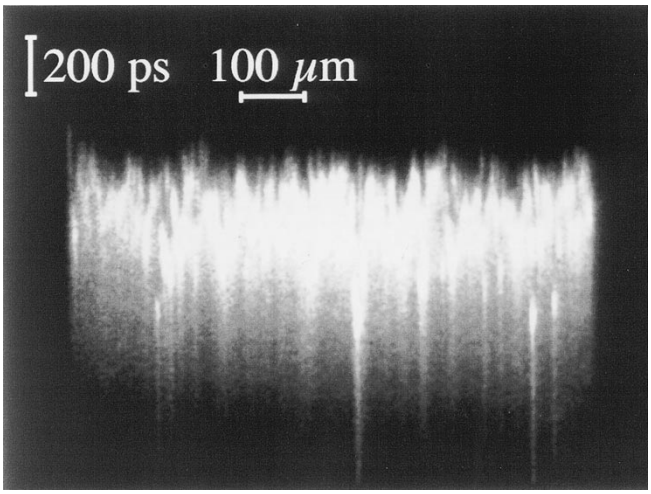

Fig. 7. Streak camera trace of optical pulses propagated through the cores traversing the diameter of the image circle.

data show the values relative to the minimum propagation delay in the area of interest. The skew ranges within 5 ps/m in the small area of 40×40 μm (about 100 cores). There was no significant difference depending on the position over the whole image circle.

By changing the magnification ratio of the objective lens, a larger number of cores can be measured. Fig. 7 shows a streak camera trace of an optical pulses propagated through the cores traversing the diameter of the image circle. By scanning the output endface, a 2-D map of time-of-flight difference all over the image circle can be plotted as shown in Fig. 8. The global distribution of measured time-of-flight difference also ranges within 5 ps/m.

From Figs. 6 and 8 the time-of-flight is distributed at random, and the skew ranges within 5 ps/m in the whole area of the image circle. With the skew of 5 ps/m, the bit rate–distance product is limited to 20 Mb/s · km. One reason for this relatively large skew compared to that of the fiber ribbon [8] is presumably due to nonuniformity of the core parameters. The test image fiber was fabricated by using some different mother-rods with different

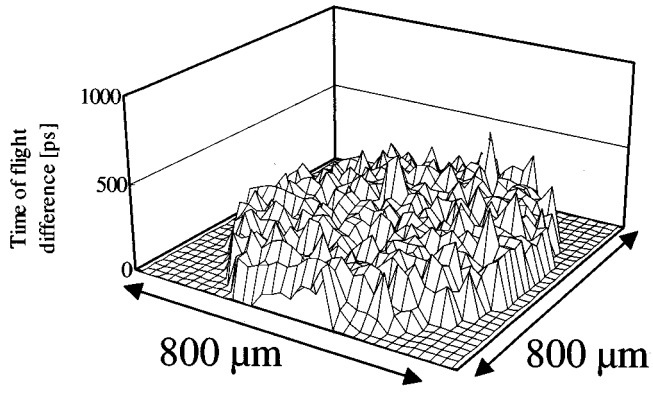

Fig. 8. Time-of-flight difference over the image circle. (Image fiber was straight.)

parameters. It is noted that this type of image fiber consisting of different cores is fabricated for conventional applications such as endoscope. The skew can be reduced by making the parameters of all the cores uniform.

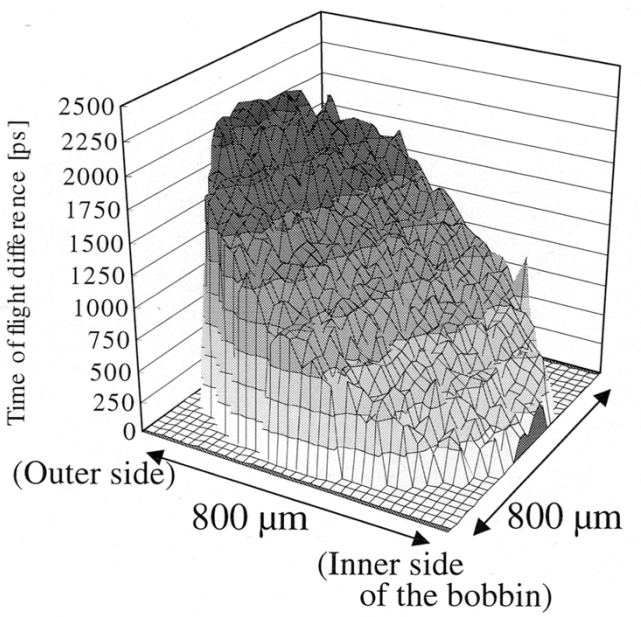

Fig. 9. Time-of-flight difference over the image circle. (Image fiber was wound by 100 turns around a bobbin.)

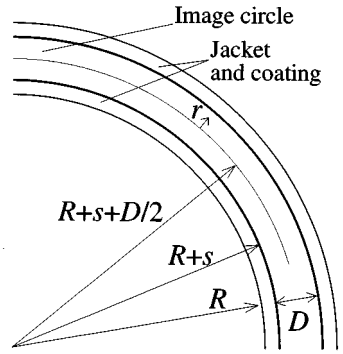

Fig. 10. Parameters of an image fiber wound around a bobbin.

V. Discussion on the Skew Due to Bending

To investigate the effect of bending on the skew, the same test 100-m-long image fiber was wound by 100 turns around a 31-cm-diameter bobbin, and skew was measured. Fig. 9 shows the measurement result. By comparing it with Fig. 8, the skew is increased monotonically toward the outer diameter by bending up to about 2 ns.

We will theoretically analyze the bending-induced skew. Assume that an image fiber is wound by m turns around a bobbin of radius R as shown in Fig. 10. The propagation delay τ due to an image fiber of length l is expressed by

$$\tau = \frac{Nl}{c} \tag{1}$$

where c and N are the speed of light in vacuum and the group index of the cores, respectively. The bending of the image fiber causes strain Δl in the axial direction and change of core refractive index Δn due to photoelastic effect. The propagation delay difference $\Delta\tau$ due to Δl and Δn is expressed as

$$\Delta\tau = \frac{N}{c}\Delta l + \frac{l}{c}\frac{\partial N}{\partial n}\Delta n. \tag{2}$$

The strain Δl on a core at a point of r is

$$\begin{aligned}\Delta l &= 2\pi m\left(R+s+\frac{D}{2}+r\right) - 2\pi m\left(R+s+\frac{D}{2}\right)\\ &= 2\pi mr\end{aligned} \tag{3}$$

where D and s are the picture diameter and the thickness of the jacket and coating of the image fiber, respectively. Next, we derive Δn. The core refractive index n under the photoelastic effect is expressed as [9], [11]

$$n = \sqrt{n_1^2 + 2n_1CW + C^2W^2} \tag{4}$$

where n_1 is the refractive index without strain, C is the lateral photoelastic constant ($C = -4.19 \times 10^{-12}$ m^2/N for silica glass), and W is the tensile stress. When the radius of curvature is larger than the minimum bending radius, $|CW/n_1| \ll 1$ is satisfied generally (see Appendix A). Therefore, from (4), the refractive index change is approximately expressed as

$$\Delta n = n - n_1 \cong CW. \tag{5}$$

Hooke's law and (3) can be used to express the tensile stress W as

$$W = \frac{\Delta l}{l}E = \frac{2\pi mr}{l}E \tag{6}$$

where E is Young's modulus ($E = 7.60 \times 10^{10}$ N/m^2 for silica glass). From (5) and (6), Δn is written as

$$\Delta n = C\left(\frac{2\pi mr}{l}E\right). \tag{7}$$

By using (2), (3), and (7), $\Delta\tau$ can be expressed as

$$\begin{aligned}\Delta\tau &= \frac{N}{c}(2\pi mr) + \frac{l}{c}\frac{\partial N}{\partial n}\cdot C\left(\frac{2\pi mr}{l}E\right)\\ &= 2\pi mr\left(\frac{N}{c}+\frac{CE}{c}\frac{\partial N}{\partial n}\right).\end{aligned} \tag{8}$$

It should be noted that the change of the propagation delay $\Delta\tau$ does not depend on the radius of the bobbin and the structural parameter of the image fiber such as the picture diameter D and thickness of jacket and coating s but it depends only on the number of turns of winding, m. Fig. 11 shows the theoretical values obtained from (8) with the experimental result. In the figure, each value is plotted by regarding a datum at the center of the image circle as a reference. It is noted that the calculated values agree well with the experimental result. The maximum difference of the propagation delay $\Delta\tau_{\max}$ occurs between the outermost and innermost parts, and it is expressed as

$$\begin{aligned}\Delta\tau_{\max} &= \Delta\tau|_{r=D/2} - \Delta\tau|_{r=-D/2}\\ &= 2\pi mD\left(\frac{N}{c}+\frac{CE}{c}\frac{\partial N}{\partial n}\right).\end{aligned} \tag{9}$$

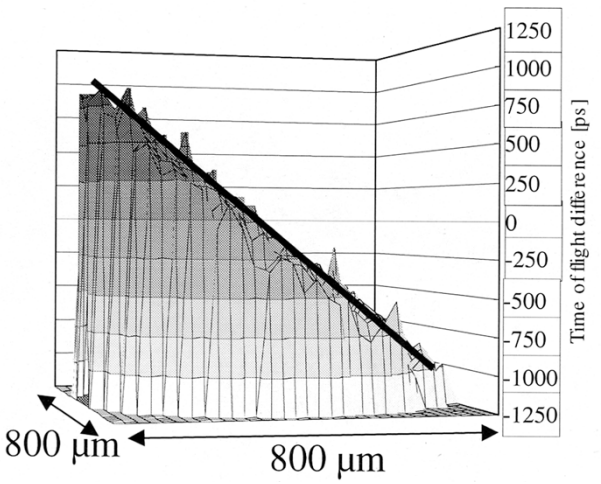

Fig. 11. Time-of-flight difference over the image circle. Theoretical data and experimental data. (Image fiber was wound by 100 turns around a bobbin.)

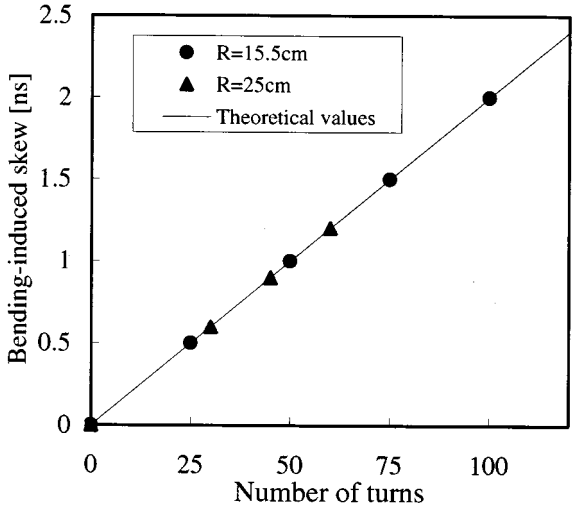

Fig. 12. Relation between number of turns and bending-induced skew.

Fig. 12 shows the theoretical values obtained from (9) and the experimental results of the bending-induced skew, plotted as a function of the number of turns. In the experiment, the test 100-m-long image fiber was wound around bobbins of different radii of $R = 15.5$ cm and $R = 25$ cm. The theoretical values agree well with the experimental results, and the bending-induced skew depends only on the number of turns m. The maximum difference of the propagation delay for one turn $\Delta\tau_1$ can be expressed as

$$\Delta\tau_1 = 2\pi D\left(\frac{N}{c} + \frac{CE}{c}\frac{\partial N}{\partial n}\right). \tag{10}$$

Here, $\Delta\tau_1$ is an intrinsic value for each image fiber and can be used to estimate the increase in skew caused by bending. The increase in skew due to winding of m turns, $\Delta\tau_{\max}(m)$, can be expressed as

$$\Delta\tau_{\max}(m) = m \times \Delta\tau_1. \tag{11}$$

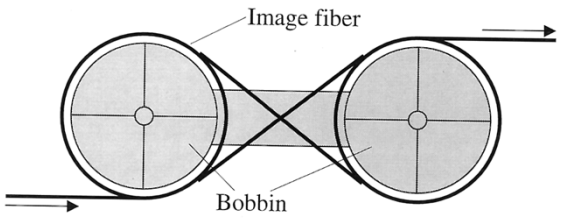

Fig. 13. An "8-shaped" bobbin for winding without increasing skew.

For the test image fiber used in the measurement above, $\Delta\tau_1 =$ 19.8 ps/turn. For example, if the test image fiber is bent by 90°, the resulting increase in skew can be calculated by using (11) as

$$\Delta\tau_{\max}(1/4) = \tfrac{1}{4} \times 19.8 = 4.95 \text{ [ps]}. \tag{12}$$

In (10), all the values except the picture diameter D barely change if the image fiber is made of silica glass. Therefore, $\Delta\tau_1$ is characterized mainly by the value of D. The picture diameter $D = 800$ [μm] of the test image fiber used in the measurement above is typical for common image fibers. Therefore, we can say that $\Delta\tau_1 \cong 20$ [ps/turn] is also typical. When an image fiber is used in the application of optical interconnects, it is expected that the winding can be restricted to less than about five turns. With this number of turns, the bandwidth limit due to bending is higher than 1 Gb/s/ch from (11). However, if the image fiber is wound around a bobbin over several tens of turns for disposal of surplus length, a large skew of over 1 ns occurs and the bandwidth is limited to less than several hundred megabits per second per channel.

One method to suppress the bending-induced skew is to twist the image fiber. When the integer multiple of the pitch of the twist is equal to the length of the bent part, the increase in skew is completely canceled. Even if this condition is not satisfied, the increase in skew can be suppressed to some extent. However, fixing an image fiber in a twisted condition at every bent part makes handling difficult. It is therefore desired to realize "*twisted image fiber*" which was previously twisted in the drawing process. Another method is to use an "*8-shaped bobbin*" proposed in Fig. 13. The surplus length of the image fiber can be disposed of without increasing skew by winding the image fiber around the bobbin in a manner to draw an"8." By using these methods, the bandwidth limit due to bending will be alleviated up to over several tens of gigabits per second per channel.

VI. Conclusion

The skew characteristics of an image fiber were investigated by using a novel measurement method. The measurement results revealed the distribution of time-of-flight difference in the image circle. To obtain high-speed transmission over 1 Gb/s/ch through a 100-m-long image fiber, the parameters of all the cores have to be made uniform. Additionally, the principle of the increase in skew due to bending was clarified.

Image fiber has been optimized for direct image transmission. Therefore, we have to re-optimize the parameters of the image

fiber for data transmission. The authors hope that this investigation will help the development of low-skew image fibers for high-throughput 2-D parallel optical interconnects.

APPENDIX

In this Appendix, we numerically explain the condition $|CW/n_1| \ll 1$. From (6), when an image fiber is wound by m turns and by bending radius R', the tensile stress W on the most stressed position $r = D/2$ can be written as

$$W = \frac{2\pi m D/2}{2\pi m R'} E = \frac{D}{2R'} E. \tag{A1}$$

Therefore, the condition can be expressed as

$$\left|\frac{CW}{n_1}\right| = \left|\frac{CED}{2n_1 R'}\right| = 0.106 \times \frac{D}{R'}. \tag{A2}$$

Here we approximately assumed $n_1 = 1.5$. In general, the picture diameter of an image fiber D is smaller than 3 mm and the minimum bending radius is lager than 30 mm. Therefore, obviously, the condition $|CW/n_1| \ll 1$ is satisfied generally.

ACKNOWLEDGMENT

The authors wish to thank T. Tsumanuma, K. Kaneda, and N. Shamoto of Fujikura Ltd. for their useful discussions. They also wish to thank W. Chujo, T. Itabe, and T. Iida of Communications Research Laboratory for their encouragement.

REFERENCES

[1] M. Ishikawa, "Optoelectronic parallel computing system with reconfigurable optical interconnection," in *SPIE Critical Review Series, Optoelectronic Interconnects and Packaging*, R. T. Chen and P. S. Guilfoyle, Eds. Bellingham, WA: SPIE Press, 1996, vol. CR62, pp. 156–175.

[2] F. A. P. Tooley, S. M. Prince, M. R. Taghizadeh, F. B. McCormick, M. W. Derstine, and S. Wakelin, "Implementation of a hybrid lens," *Appl. Opt.*, vol. 34, no. 28, pp. 6471–6480, 1995.

[3] K. Hamanaka, "Optical bus interconnection system using Selfoc lenses," *Opt. Lett.*, vol. 16, no. 16, pp. 1222–1224, 1991.

[4] K. Kitayama, "Novel spatial spread spectrum based fiber optic CDMA networks for image transmission," *IEEE J. Select. Areas Commun.*, vol. 12, pp. 762–772, 1994.

[5] K. Kitayama, M. Nakamura, Y. Igasaki, and K. Kaneda, "Image fiber-optic two-dimensional parallel links based upon optical space-CDMA: Experiment," *J. Lightwave Technol.*, vol. 15, pp. 202–212, Feb. 1997.

[6] M. Nakamura, K. Kitayama, Y. Igasaki, and K. Kaneda, "Four-channel, 8×8 bit, two-dimensional parallel transmission by use of space-code-division multiple-access encoder and decoder modules," *Appl. Opt.*, vol. 37, no. 20, pp. 4389–4398, July 1998.

[7] M. Nakamura, K. Kitayama, Y. Igasaki, and K. Kaneda, "Space-CDMA based 2D parallel optical transmission over record length (100 m) long image fiber," *Electron. Lett.*, vol. 34, no. 11, pp. 1127–1128, 1998.

[8] A. P. Kanjamala and A. F. J. Levi, "Subpicosecond skew in multimode fiber ribbon for synchronous data transmission," *Electron. Lett.*, vol. 31, no. 16, pp. 1376–1377, 1995.

[9] N. Kashima, "Influence of fiber parameters on skew in single-mode fiber ribbons," *J. Lightwave Technol.*, vol. 15, no. 10, pp. 1858–1864, 1998.

[10] S. Kawai, Y. Li, and T. Wang, "Skew-free optical interconnections using fiber image guides for petabit-per-second computer networks," *Japan J. Appl. Phys.*, vol. 37, no. 6B, pp. 3754–3758, 1998.

[11] J. Sakai and T. Kimura, "Birefringence and polarization characteristics of single-mode optical fibers under elastic deformations," *IEEE J. Quantum Electron.*, vol. QE-17, pp. 1041–1051, June 1981.

Moriya Nakamura (M'96) received the B.E. and M.E. degrees in electrical engineering from the Science University of Tokyo, Japan, in 1991 and 1993, respectively.

In 1993, he joined the Communications Research Laboratory, Ministry of Posts and Telecommunication, Tokyo. His main research interests are in optical interconnection, image fiber optics, and fiber-optic CDMA.

Mr. Nakamura is a member of the Institute of Electronics and Information Communication Engineers (IEICE) of Japan.

Toshimichi Otsubo was born in Fukuoka, Japan, in 1970. He graduated from the Faculty of Law, Hitotsubashi University, Japan, in 1993.

Since 1993, he has been employed by the Communications Research Laboratory, Ministry of Posts and Telecommunication, Tokyo, Japan. Since 1998, he has been a visitor at the NERC Space Geodesy Facility (Monks Wood), U.K. He has worked on the developmet of laser ranging systems and data analysis software for space geodetic technology.

Ken-ichi Kitayama (S'75–M'76–SM'89) received the B.E., M.E., and Dr.Eng. degrees in communication engineering from Osaka University, Osaka, Japan, in 1974, 1976, and 1981, respectively.

In 1979, he joined the NTT Electrical Communication Laboratory, where he was engaged in research on fiber optics. During the academic year 1982–1983, he studied semiconductor lasers and integrated optics at the University of California at Berkeley, as a Visiting Scholar. In 1987, he initiated research on optical signal processes at the NTT Transmission Systems Laboratories. In 1995, he joined the Communications Research Laboratory, Ministry of Posts and Telecommunication of Japan, Tokyo. Since 1999, he has been with the Osaka University, Osaka, Japan, where he is currently Professor in the Department of Electronic and Information Systems in the Graduate School of Engineering. His research interests are in photonic networks and fiber-optic wireless access networks. He has published over 140 papers in refereed journals, has written two book chapters, and translated on book from English into Japanese. He has been awarded about 40 patents.

Dr. Kitayama serves as the Associate Editor of the IEEE PHOTONICS TECHNOLOGY LETTERS. He received the 1980 Young Engineer Award from the Institute of Electronics and Communication Engineers of Japan, and the 1985 Paper Award of Optics from the Japan Society of Applied Physics. He is a member of the Institute of Electronic, Information, and Communication Engineers of Japan, the Japan Society of Applied Physics, and the Optical Society of Japan.